STEM CELLS AND DEVELOPMENT
Volume 22, Number 21, 2013

DOI: 10.1089/scd.2012.0718

Isolation and Characterization of a Spontaneously Immortalized Multipotent Mesenchymal Cell Line Derived from Mouse Subcutaneous Adipose Tissue

Andrea Zamperone,[1,*] Stefano Pietronave,[1,*] Simone Merlin,[1] Donato Colangelo,[1] Gabriella Ranaldo,[1] Enzo Medico,[2,3] Federica Di Scipio,[4] Giovanni Nicolao Berta,[4] Antonia Follenzi,[1,5] and Maria Prat[1,5]

The emerging field of tissue engineering and regenerative medicine is a multidisciplinary science that is based on the combination of a reliable source of stem cells, biomaterial scaffolds, and cytokine growth factors. Adult mesenchymal stem cells are considered important cells for applications in this field, and adipose tissue has revealed to be an excellent source of them. Indeed, adipose-derived stem cells (ASCs) can be easily isolated from the stromal vascular fraction (SVF) of adipose tissue. During the isolation and propagation of murine ASCs, we observed the appearance of a spontaneously immortalized cell clone, named m17.ASC. This clone has been propagated for more than 180 passages and stably expresses a variety of stemness markers, such as Sca-1, c-kit/CD117, CD44, CD106, islet-1, nestin, and nucleostemin. Furthermore, these cells can be induced to differentiate toward osteogenic, chondrogenic, adipogenic, and cardiogenic phenotypes. m17.ASC clone displays a normal karyotype and stable telomeres; it neither proliferates when plated in soft agar nor gives rise to tumors when injected subcutaneously in NOD/SCID−γ^{null} mice. The analysis of gene expression highlighted transcriptional traits of SVF cells. m17.ASCs were genetically modified by lentiviral vectors carrying green fluorescent protein (GFP) as a marker transgene and efficiently engrafted in the liver, when injected in the spleen of NOD/SCID−γ^{null} monocrotaline-treated mice. These results suggest that this non-tumorigenic spontaneously immortalized ASC line may represent a useful tool (cell model) for studying the differentiation mechanisms involved in tissue repair as well as a model for pharmacological/toxicological studies.

Introduction

Adult stem cells are present in most of the tissues and exhibit self-renewal and multipotency, contributing to tissue homeostasis. Among adult stem cells, the mesenchymal ones have a greater availability and plasticity, likely candidating them for applications in regenerative medicine [1]. These cells were originally isolated from bone marrow and, more recently, from the stromal vascular fraction (SVF) of adipose tissue [2]. This is an attractive stem cell source because of the simple and repeatable access to adipose tissue, the basic enzyme-based isolation procedures, and the relatively larger available stem cell amounts compared with bone marrow [3–6]. Several comparative studies have shown that adipose-derived stem cells (ASCs) and those from bone marrow display similar properties with regard to cell-surface expression profile, differentiation potential, and therapeutic efficacy [7–11]. The SVF at early passages is composed of a heterogeneous cell population consisting, besides stem cells, also of endothelial, smooth muscle cells, pericytes, fibroblasts, mast cells, and pre-adipocytes [3–5,12]. It should be noted that within a few in vitro passages, a relatively homogeneous population of ASCs can be isolated. Although antigenic identity of this cell population remains controversial, there is a general consensus for the expression of a set of surface markers, such as Sca-1, c-kit/CD117, CD44, CD90, CD73, CD29, CD105, and the absence of CD31 [3–5,10,13].

Despite ASCs having been studied for more than 10 years, some aspects for their use in a safe regenerative medicine still require further investigation [5,14,15]. In particular, due to their stem nature, concerns have arisen on their possible tumorigenic potential [16–18], which can be unleached if cells stand long-term culture, and is generally accompanied by chromosomal instability [19–22]. It has been suggested

[1]Dipartimento di Scienze della Salute, Università del Piemonte Orientale, Novara, Italy.
[2]Institute for Cancer Research @ Candiolo, Candiolo, Italy.
[3]Dipartimento di Oncologia and [4]Dipartimento di Scienze Cliniche e Biologiche, Università di Torino, Torino, Italy.
[5]Centro di Biotecnologie per la Ricerca Medica Applicata (BRMA), Novara, Italy.
*These two authors contributed equally to the work.

that this risk could be reduced, or even abolished, when stem cells are induced toward differentiation [23]. Although many in vitro differentiation protocols have been established, at present, this field is still under active investigation. For example, stem cells can now be used in cell therapy applications to obtain cell sheets or 3D proto-tissues under controlled conditions [24–29]. The latter are dictated by different local environment factors, such as growth-differentiation factors, adhesive molecules within the extracellular matrix, the properties of a possible supporting scaffold, as well as genetic programming and stochastic events [30–40]. All these studies may require a significant amount of primary cells and an extensive in vitro expansion, but ASCs generally undergo "replicative senescence" and irreversible growth arrest after a few replication cycles [20]. Alternatively, these cells can stand long-term culture, but are affected by chromosomal instability and loose multipotency, making them not suitable for regenerative medicine application [41]. The availability of a stable cell line model could facilitate studies that are aimed at describing the contribution of different factors in tissue plasticity, would add knowledge in the field of multipotent stem cell differentiation, and, moreover, could also be used to investigate its pharmacological modulation.

Here, we report the characterization of a spontaneously immortalized cell line, named m17.ASC, derived from adipose tissue of adult FVB/N mice. This cell line expresses stemness markers, has a normal karyotype, is devoid of transforming and tumorigenic potential, and, most interestingly, is multipotent. When compared with SVF, m17.ASCs display a similar gene expression profile. Furthermore, when green fluorescent protein (GFP)-transduced m17.ASC cells were injected in the spleen of NOD/SCID$-\gamma^{null}$ mice, they efficiently engrafted in the liver of transplanted mice, candidating this cell line as a valuable stemness model.

Materials and Methods

Cell isolation, cloning, culturing, and transduction

SVF was isolated from minced s.c. and epididymal/parametrial fat pads of 11-week-old mice (FVB/N strain; Charles River) and digested with 0.1% type I collagenase (Worthington Biochemical) in phosphate-buffered saline (PBS) at 37°C for 1 h. After filtration through 30-μm strainers (MiltenyiBiotec GmbH) and centrifugation for 10 min at 1,500 rpm at 4°C, floating adipocytes were removed, and the SVF pellet was treated with erythrocyte lysis buffer (154 mM NH_4Cl, 20 mM Tris pH 7.5). Cells were sorted by an immunomagnetic procedure with Sca-1 antibodies (MiltenyiBiotec) and plated in Claycomb medium (Sigma-Aldrich), supplemented with 2 mM L-glutamine, 10% fetal bovine serum (FBS; Lonza Ltd.), 100 IU/mL penicillin, and 100 μg/mL streptomycin. Cells were regularly split when subconfluent at a ratio of 1/3, and medium was changed every 2–3 days. After the second passage, some cells were plated at a low density (50–200 cells/cm^2). A single cell colony was detected after 1 week by microscope inspection, which was then grown and cloned twice. This cell line (m17.ASC) can be passaged at 1/8–1/10 every 3 days. Population doubling time, calculated by using the formula from Cristofalo et al. [42], as well as telomere length was evaluated in a 32 day time span. For this analysis, m17.ASC (1×10^5/cm^2) were sequentially transplanted every 3 days. In parallel, the same procedure was adopted for freshly isolated primary cells at p1, which were used as reference. m17.ASCs were transduced with a Lentiviral Vector for the expression of GFP under the control of the phosphoglycerate kinase promoter. L929 fibroblasts (ATCC CRL-2148), NIH-3T3 (ATCC, CRL-1658^{TM}), and NIH-3T3-MET-EC$^-$ were also used [43].

Cytofluorimetric analysis

Cells, detached with 5 mM EDTA, were incubated for 20 min on ice with PE-labeled anti-Sca-1, anti-c-kit (anti-CD117) (Biolegend), anti-CD90 (ImmunoTools), or fluorescein isothiocyanate (FITC)-labeled anti-CD44, CD106, CD-31, CD34, CD45, and F4/80 antibodies (Biolegend), as suggested by the manufacturer's indications. Cells were fixed in buffered 1% paraformaldehyde (PAF), 2% FBS and analyzed in an FACScalibur flow cytometer (BD Biosciences).

RT-PCR analysis

Total cell RNA was extracted in Trizol® reagent (Invitrogen), followed by DNase treatment (DNAse I; Fermentas). Then, 1 μg of RNA was retrotranscribed in cDNA with the RevertAid™ H Minus First-Strand cDNA Synthesis Kit (Fermentas) using oligo(dT) primers. PCRs were performed using the PCR Master Mix 2× kit (Fermentas) in a final volume of 25 μL containing 50 ng cDNA and 200 nM primers (listed in Table 1). PCR conditions were as follows: 94°C 2 min, 35 cycles 94°C for 30 s, specific annealing temperature for 30 s (see Table 1), 72°C for 30 s, and 72°C for 7 min. Twenty-five cycles were performed for *GAPDH*. The amplified products were resolved by 2% agarose gel electrophoresis, stained with ethidium bromide, and documented with GelDoc system (Bio-Rad Laboratories). The quantitative RT-PCR was performed on the cDNA from control and differentiated cells in a 20-μL total volume containing 1× SYBR green PCR master mix (Promega), 0,5 ìM forward and reverse primers, and 50 ng of cDNA. Quantitative PCR was performed by incubation at 95°C for 3 min and 40 amplification cycles at 95°C for 15 s and then at 60°C for 1 min.

Telomere length determination

Genomic DNA was extracted with Gres whole-blood DNA extraction kit (InCura). Real-time PCR was used to assess average telomere length ratio. Telomeric DNA amount was normalized to that of the acidic ribosomal phosphoprotein PO *(36B4)*, as a housekeeping gene. The analysis was based on Callicot method [44]. Briefly, telomere assay was performed in triplicate for each treatment in a 25 μL reaction volume containing 20 ng genomic DNA, 12.5 μL EVA Green SMX (Bio-Rad Laboratories), 300 nM each of forward and reverse primers for telomeres, and 300 and 500 nM forward and reverse primers for 36B4, in an automated CFX96 thermocycler (Bio-Rad Laboratories). The reaction conditions for telomere were 95°C for 10 min followed by 30 cycles of data collection at 95°C for 15 s and a 56°C anneal–extend step for 1 min. For the *36B4* portion, the reaction conditions were set at 95°C for 10 min followed by 35 cycles of data collection at 95°C for 15 s, with 52°C annealing for 20 s, followed by extension at 72°C for 30 s.

Results were analyzed with Bio-Rad CFX Manager and exported to Excel (Microsoft) for calculation. For each data

Table 1. Primers Used for the DNA Amplification of Specific Target Genes

Target gene	*Forward sequence*	*Reverse sequence*	*Fragment size (bp)*	*Annealing (°C)*
Sca-1	5′-ACTGTGCCTGCAACCTTGTCTGAGA-3′	5′-GTCCAGGTGCTGCCTCCATT-3′	322	62
c-kit	5′-GCCCTAATGTCGGAACTGAA-3′	5′-TTGCGGATCTCCTCTTGTCT-3′	319	60
Nucleostemin	5′-GGGAAAAGCAGTGTCATTA-3′	5′-GGGATGGCAATAGTAACC-3′	405	54
Islet-1	5′-GCCTCAGTCCCAGAGTCATC-3′	5′-AGAGCCTGGTCCTCCTTCTG-3′	308	60
Nestin	5′-TCAAGGGGAGGCCAGGAAGGA-3′	5′-CTGCAGCCCCACTCAAGCCATC-3′	425	66
GAPDH	5′-ATCACTGCCACCCAGAAGACT-3′	5′-ATCGAAGGTGGAAGAGTGGGA-3′	350	60
Adiponectin	5′-AGCCGCTTATGTGTATCGCT-3′	5′-GAGTCCCGGAATGTTGCAGT-3′	150	60
Osteocalcin	5′-GCAATAAGGTAGTGAACAGACTCC-3′	5′-GTTTGTAGGCGGTCTTCAAGC-3′	120	66
Aggrecan	5′-CCCTCGGGCAGAAGAAAGAT-3′	5′-CGCTTCTGTAGCCTGTGCTTG-3′	150	60
β-Actin	5′-GATGACCCAGATCATGTTTGAGA-3′	5′-GTCTCCGGAGTCCATCACAAT-3′	120	60
Telomere	5′-CGGTTTGTTTGGGTTTGGGTTTGG GTTTGGGTTTGGGTT-3′	5′-GGCTTGCCTTACCCTTACCCTTAC CCTTACCCTTACCCT-3′		
36B4	5′-ACTGGTCTAGGACCCGAGAAG-3′	5′-TCAATGGTGCCTCTGGAGATT-3′		

point, a T/S value was calculated: Threshold cycle values (Ct) were determined from semilog amplification plots (log increase in fluorescence versus cycle number) for telomere (T) and *36B4* gene (S). The relative ratio of telomere repeat copy number to the *36B4* single copy gene copy number (T/S ratio) for each time point was calculated as: $[2^{Ct(telomere)}/2^{Ct(36B4)}]^{-1}=2^{-\Delta Ct}$, and related to the primary cell line telomere T/S at passage 3 by using the formula: $2^{-(\Delta Ct\ m17.ASC\_\Delta Ct\ primary)}=2^{-\Delta\Delta Ct}$ (Fig. 3c; $P>0.1$). Samples with a T/S >1.0 had an average telomere length ratio greater than that of the primary cell line.

Differentiation protocols

Cells were plated onto 35 mm dishes (2×10^4 cells/cm^2) and cultured in adipogenic medium (Lonza) or osteogenic medium (DMEM, FBS 10%, 50 μg/mL ascorbic acid, 10 mM β-glicerophosphate, and 10 nM dexamethasone), which were changed every 3 days. After 14–20 days, cells were washed in cold PBS, fixed with 4% PFA in PBS, and stained with Adipored (Lonza) or 40 mM alizarin red S, pH 4.1 [45]. The presence of lipid vacuoles was visualized under a fluorescence microscope, while the production of calcium deposits was examined in light microscopy. For chondrogenic differentiation, 2.5×10^5 cells were cultured as a "pellet" for 40 days in 15 mL centrifuge tubes in chondrogenic differentiation medium (Lonza). The medium was changed every second day. Cells were then washed, fixed as described earlier, included in OCT (Fisher), and frozen at −80°C. Five-micrometer sections were cut, fixed again as earlier, washed, stained with 1% Alcian blue in 3% acetic acid, pH 2.5 for 30 min, and observed under a light microscope. Sections were also fixed in 3% PAF for 20 min, stained with goat antibody against collagen II (Santa Cruz Biotechnology, Inc.; 1:200), in PBS, 1% bovine serum albumin (BSA), and 2% FBS for 2 h at room temperature, followed by secondary Alexa Fluor® 546 donkey-anti-goat-IgG antibody (Invitrogen; 1:500) for 45 min at room temperature. Nuclei were stained with TO-PRO3 (Invitrogen; 1:100) and observed by a Leica SP2 laser scanning confocal microscope. For cardiomyogenic differentiation, m17.ASC were co-cultured with neonatal cardiomyocytes (nCMs) isolated from hearts of 1–3-day-old FVB/N mice, as indicated in the manufacturer's instructions (kit by Worthington Biochemical Corp.). Briefly, immediately after isolation, cells were pre-plated for 2 h 30 min to recover the non-adherent-enriched fraction of nCMs, which were then seeded on fibronectin (2 μg/mL; Sigma-Aldrich), laminin (0.2%), gelatin (0.02%) pre-coated plates or pre-coated glass chamber slides (BD Biosciences). m17.ASC, labeled with DIIC12(3) fluorescent dye (BD Bioscences), were seeded directly onto nCMs (1:10 ratio) in complete medium, and co-cultures were carried on for 7 days. m17.ASC and nCMs alone were used as negative controls. Co-cultures were also set up with cells isolated from the SVF at their second passage and nCMs. Cells were fixed in 3% PAF for 20 min, permeabilized in 0.2% Triton ×100 in PBS for 10 min, and incubated with rabbit antibodies against GATA-4 (1:400), MEF2c (1:100) (Abcam), or monoclonal antibodies against Troponin T and alpha sarcomeric actinin (Abcam; 1:100), in PBS, 1% BSA, and 4% FBS for 2 h at room temperature, followed by secondary Alexa Fluor 488 goat-anti-rabbit-IgG antibody or secondary goat-anti-mouse FITC-labeled antibodies (Abcam; 1:500) for 45 min at room temperature. Nuclei were counter-stained with DAPI (Sigma-Aldrich; 1:200) and observed by a Leica DMI6000B microscope. Positive cells were counted in at least 12 independent fields against total nucleated cells.

Karyotype analysis

Chromosomal analysis of m17.ASCs was carried out starting from passage 10, every 10 passages, till passage 108, as previously described [46]. Briefly, cells undergoing active division were blocked at metaphase by colchicine and actinomycin D, detached, and centrifuged, and the pellet was resuspended in hypotonic solution (0.075 M potassium chloride). Cells were then fixed in Carnoy fixative and stained with 0.06% Wright's stain (Sigma-Aldrich) pH 6.8. Unmounted slides were examined using Nikon Eclipse 1000 light microscopy and photographed with Genicon software. Thirty high-quality G-banded metaphases were selected each time. The chromosomes were classified according to the Standard Karyotype of the Mouse (Committee On Standardized Genetic Nomenclature For Mice, 1972) [47].

Analysis for anchorage-independent proliferation

Cells (5×10^3/well) were seeded in 12-well plates in semisolid medium (0.3% agar-Agar Noble; Sigma-Aldrich, in

DMEM 2% FCS). NIH-3T3 and NIH-3T3-Met^{EC-} cells were used as negative and positive controls [43]. Medium was replaced weekly. After 3 weeks, the colonies were stained with MTT [3-(4,5-dimethylthiazol-2-yl)-2,5-diphenyl tetrazolium bromide; Sigma-Aldrich], photographed with Versadoc imager (Bio-Rad Laboratories), and counted with Quantity One colony counting software (Bio-Rad).

Gene expression analysis

Total RNA was extracted using miRNeasy kit (Qiagen) and quality controlled using a Bioanalyzer 2100 (Agilent Technologies). Microarray analysis was performed using MOUSEWG-6_V2 Beadchips (Illumina), according to standard protocols. Raw data were processed and cubic-spline normalized using the GenomeStudio software (Illumina). An analysis for the selection of differentially expressed genes and dot plot generation was carried out with Excel (Microsoft).

In vivo experiments

For the tumorigenicity assay, 5×10^6 GFP-m17.ASC cells at passage 120 were injected subcutaneously into the posterior flank of 5 NOD/SCID-γ^{null} female mice. Two$\times10^6$ of B16 murine melanoma cells, and of A549 human lung adenocarcinoma cells were injected as positive controls. Mice were inspected twice a week for approximately 10 weeks.

For the engraftment experiments, six seven-week-old NOD/SCID-γ^{null} male mice were treated with monocrotalin (200 mg/kg, i.p. injection; Sigma-Aldrich), a toxic pyrrolizidine alkaloid of plant origin causing lung and liver endothelial injury, and the next day, 2×10^6 GFP-m17.ASC were infused by an intrasplenic injection [48]. The animals were observed daily, and killed at different time points (from 1 week up to 6 weeks) after cell injection. Livers were fixed in 4% PAF, embedded in OCT, and frozen in liquid nitrogen-precooled isopenthane. Cryostat sections (5 μm thick) were postfixed with 4% PAF, blocked with 5% goat serum (Vector Laboratories), 1% BSA, and 0.1% Triton X-100 in PBS, and incubated with rabbit anti-GFP (Invitrogen; 1:400) and rat anti-CD31 antibodies (BD Pharmigen, BD Biosciences; 1:50), followed by Alexa Fluor 488 goat anti-rabbit IgG and Alexa Fluor 546 goat anti-rat IgG (Invitrogen; 1:500) secondary ones, respectively, and TO-PRO3 (Invitrogen). Tissue sections were observed under a Leica SP2 laser scanning confocal microscope. All procedures were carried out in accordance with the European Community Directive for Care and Italian Laws on animal experimentation (Law by Decree 116/92).

Statistical analysis

The results are shown as mean ± standard deviation, and significance was calculated by unpaired *t*-test. The values are considered significantly different when $p < 0.05$. The number of replicated experiments performed is given as *n*.

Results

Characterization of the m17.ASC clone

Cells isolated from the SVF of s.c. adipose tissue after immunomagnetic selection for Sca-1 appeared as a homogeneous population that was highly positive for Sca-1 in immunofluorescence. Sca-1 expression in this cell population declined after a few passages, and cells generally displayed morphological signals of senescence and stopped proliferating after 7–9 passages. At the second passage, cells were plated sparsely (50–200 cells/cm^2 for a total of 180 cm^2), and a colony emerged from a single cell. This original colony was cloned twice, and it has been propagated since then for more than 2 years of continuous culture and named m17.ASC. It displays a fibroblast-like morphology (Fig. 1a). m17.ASCs were constantly analyzed for the expression of different stemness markers, namely Sca-1, c-kit, Islet 1, nestin, and nucleostemin in RT-PCR (Fig. 1b), and no differences were observed at the different passages. They were constantly positive for all these markers. By contrast, cells from primary culture (SVF), which at the beginning expressed the same markers, although some (nestin and nucleostemin) at lower levels, displayed the tendency to lose their expression from the very first passages. The expression of the embryonic stemness cell markers Nanog, Oct4, Sox2, Klf4, and Myc was found to be negative (Nanog, Oct4), very low (Sox2), or medium-low (Klf4, Myc) with both RT-PCR and microarray analysis (data not shown). Cytofluorimetric analysis confirmed the expression of Sca-1 and c-kit/CD117 in m17.ASC cells (Fig. 1c, d). Moreover, these cells also expressed the mesenchymal markers CD44, CD106 at high levels and CD90 at moderate levels. They were negative for the endothelial marker CD31, the leukocyte markers CD34 and CD45, and the macrophage marker F4/80. The L929 fibroblasts, used as control, do not express any of the stemness markers, except nucleostemin (Nst).

The m17.ASC line displays multipotency and can be driven toward the cardiomyogenic phenotype

This spontaneously immortalized cell line displayed the multilineage potential of MSC. Indeed, when cultured in appropriate differentiation media, m17.ASCs acquired features of the osteogenic, adipogenic, and chondrogenic phenotypes, as they were specifically stained with alizarin red, adipo-red and Alcian blue, and the tissue-specific collagen II antibodies, respectively (Fig. 2a). Moreover, a quantitative RT-PCR analysis showed that the respective lineage markers osteocalcin, adiponectin, and aggrecan were up-regulated on the differentiation treatments (Fig. 2b).

In view of the fact that in regenerative medicine, cells with cardiomyogenic properties may be particularly interesting, we focused on the possibility of driving m17.ASC multipotency toward a cardiomyogenic phenotype. When co-cultured with murine nCMs, DIIC12(3)-labeled m17.ASCs displayed a marked up-regulation of GATA-4 and de novo expression of Mef2c (Fig. 2c, d). In addition, adherent cells from the SVF of adipose tissue, from which the m17.ASC clone was derived, became positive for the expression of GATA-4 and MEF2c, when co-cultured with nCMs with a similar efficiency (Fig. 2c). In the same kind of experiment, a few co-cultured DilC12(3)-labeled m17.ASCs acquired the expression of alpha-sarcomeric actin and troponin T (Fig. 2d). Altogether, these results indicate that m17.ASC have the same multipotency as the bulk population from which they were derived.

Karyotypic analysis of the m17.ASC line

m17.ASC G-banding analysis did not reveal any macroscopic chromosome alterations of cultured cells over time, if

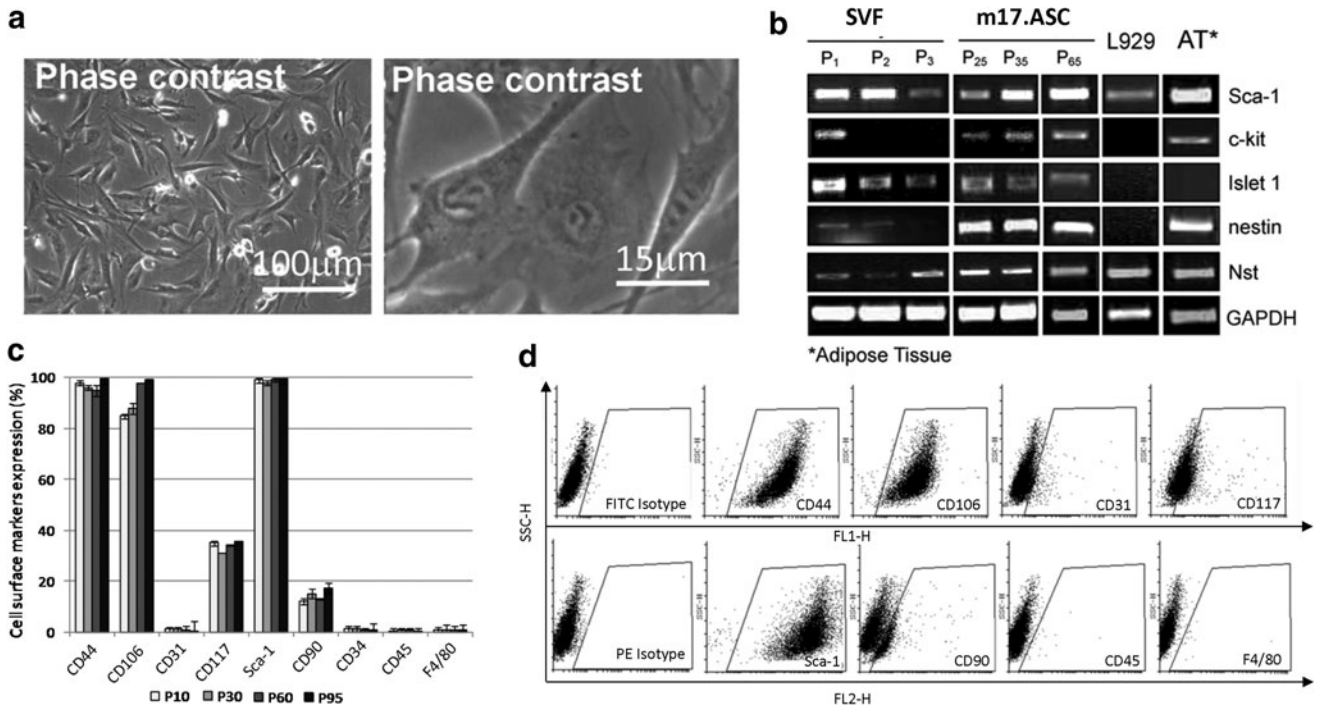

FIG. 1. Properties of the clonal cell line m17.ASC. Morphology of the m17.ASC clone, which was generated from Sca-1 + cell cultures plated at low density (200 cells/cm^2) at the phase-contrast microscope at two different enlargements **(a)**. Phenotype of m17.ASCs, characterized in RT-PCR **(b)** and cytofluorimetry **(c, d)** for different stemness markers at different passages. The clone has a fibroblast-like aspect and continues to express stemness markers with time. Representative experiments out of the three performed are reported. SVF, cells from stromal vascular fraction; ASC, adipose derived stem cells.

compared with normal mouse karyotypes. Cell karyotype analysis performed on three different in vitro passages: p10 and p73 is depicted (Fig. 3a). Analysis at passage 108 gave identical results (not shown).

Cell duplication and telomere length

Population doubling time and telomere length were evaluated in m17.ASC sequentially at several times. Both the clone, which was analyzed from passage 82 to passage 91 (p82–p91), and the primary cultures, which were analyzed from p1 to p10, displayed a constant doubling time of 32 h till the fifth passage (Fig. 3b). After this passage, the doubling time of m17.ASC remained stable, while primary cells showed a progressive increase. In this sequence of passages (p82–91) of m17.ASC cells, as well as in others (from passage 27 to passage 32, from passage 43 to passage 49, and from passage 107 to passage 113), telomere length was evaluated and compared with that of the primary cells (SVF) at passage 1. Telomeres displayed a variable length, but the overall mean length was rather constant throughout p27 to p113, displaying a variability within ±40%, when compared with reference SVF at p1. This behavior is in line with that which is also reported in other systems, such as germinal cells with a modulated telomerase activity.

The m17.ASCs maintain the properties of a normal immortalized cell line, and do not display a transformed or a tumorigenic phenotype

Cell immortalization is often accompanied by transformation and acquisition of a tumorigenic phenotype. m17.ASC cells were tested for the ability to grow in anchorage-independent conditions and thus plated in soft agar. Cultures were monitored for 21 days: The monitored m17.ASC colonies were in the same range of those obtained from the NIH-3T3 negative control (Fig. 3d). By contrast, transformed NIH-3T3-Met-EC$^-$, which were used as positive controls, gave a significantly higher number of colonies. To further corroborate this in vitro finding, cells were tested for their ability to form tumors in NOD/SCID-γ^{null} mice, which are immunocompromised, enabling the growth of allo- and xeno-tumors. In the five animals, the GFP-m17.ASC-injected cells could not induce a tumor in a period of 10 weeks. By contrast, B16 murine melanoma cells and A549 human lung adenocarcinoma cells induced the formation of tumors within 2 weeks after a cell injection. In these cases, animals had to be killed for ethical reason before 4 weeks (tumors bigger than 2 cm in the two measured directions) (data not shown). It can, thus, be concluded that this cell line behaves similarly to a normal immortalized cell line and is devoid of transforming or oncogenic potential.

Global gene expression

Global gene expression profiles obtained with DNA microarrays revealed that m17.ASCs and SVF cells have closely related transcriptomes ($R^2 = 0.805$) (Fig. 4a). However, a fraction of genes displayed cell-specific expression, defined as significant detection P value only in one of the two cell types, and different thresholds of fold change. When the threshold was set at a 3-fold gain, out of 45,281 probe sequences analyzed, 414 gave signals only in SVF cells and 235 only in m17.ASC, which became 82 and 23, respectively, for a threshold of

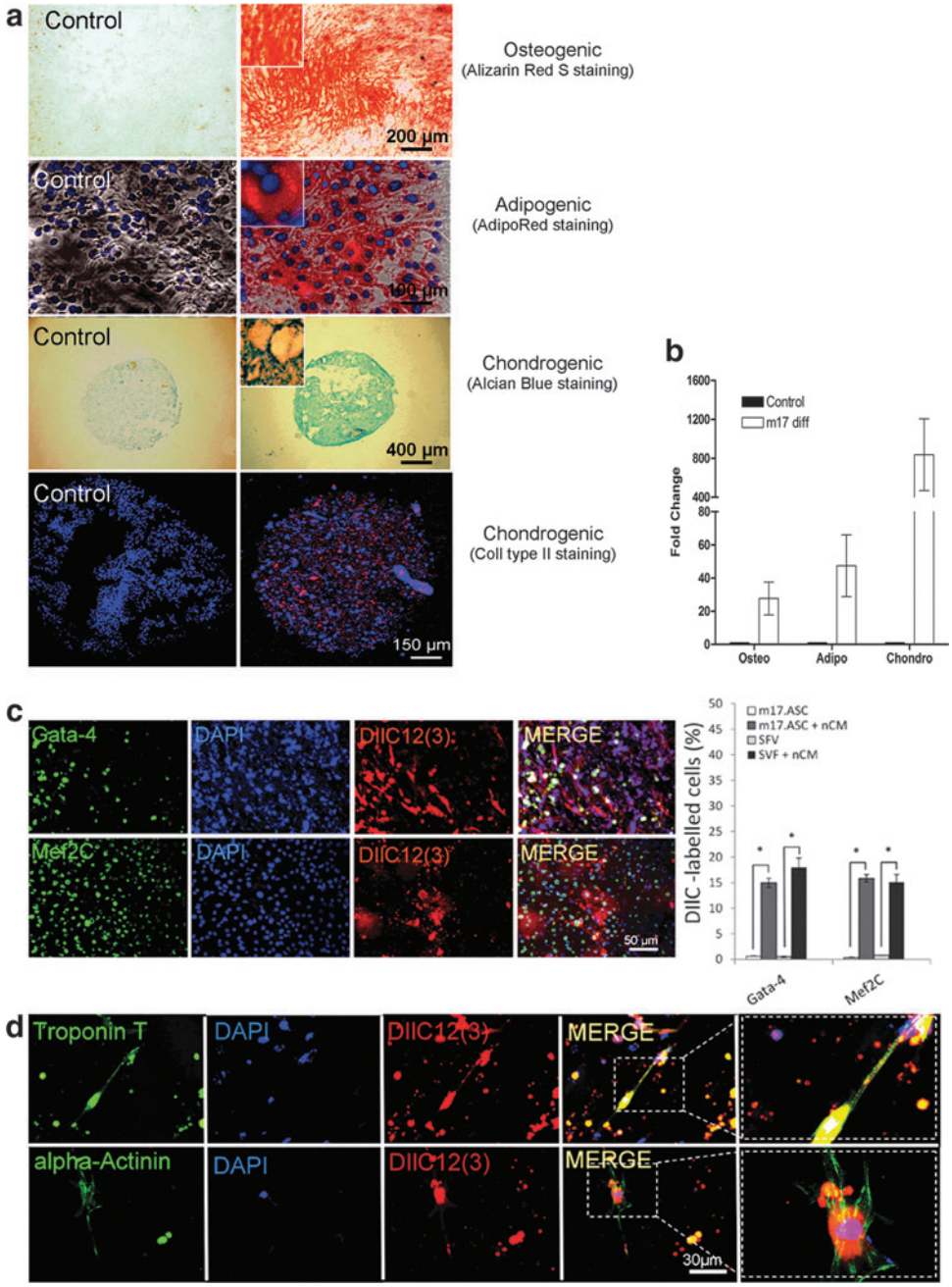

FIG. 2. The m17.ASCs are multipotent and can be induced toward a muscle/cardiac phenotype. **(a)** Cells were cultured in normal expansion medium (*left*) or in appropriate media as for specific differentiation (from *top* to *bottom*) toward osteogenic (alizarin red), adipocytic (Adipored), and chondrogenic (Alcian blue and collagen II) phenotypes (*right*); **(b)** quantitative RT-PCR was performed for differentiation markers (osteocalcin, adiponectin, and aggrecan), respectively; values represent the mean ± SD gene expression measure from three independent experiments. **(c)** DiIC12(3)-labeled m17.ASCs (*red*) were co-cultured with nCMs for 7 days, then fixed, permeabilized, immunostained for GATA-4 or MEF2c (*left panels*: *green*), counter-stained with DAPI (*blue*), and examined under a fluorescence microscope, singly or after merging (*right panels*). Quantification of DiIC12(3)-labeled m17.ASCs and SVF-differentiated cells after a 7 day co-culture. The results are shown as mean ± SD and are obtained by counting 12 independent fields at 10× magnification ($n = 3$). At least 500 DIIC12(3)-labeled cells were counted in each of the three experiments performed. $^*p < 0.05$, Student's t test. **(d)** DiIC12(3)-labeled m17.ASCs (*red*) were co-cultured, fixed, permeabilized as described earlier, and immunostained for alpha-cardiac actinin or cardiac Troponin T (*left panels*: *green*) or DAPI (*blue*) and examined under a fluorescence microscope, singly or after merging (*right panels*). Representative experiments out of the three performed are reported. SVF, stromal vascular fraction; nCM, neonatal cardiomyocytes. Color images available online at www.liebertpub.com/scd

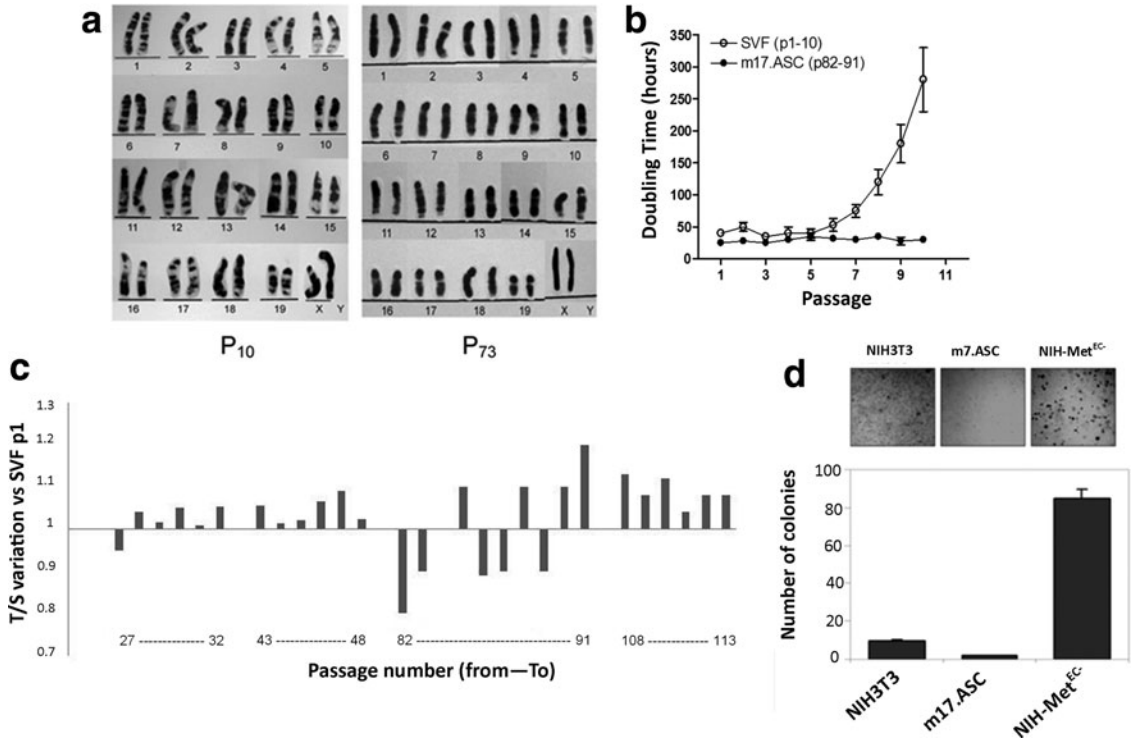

FIG. 3. m17.ASCs have a normal immortal phenotype. **(a)** Karyotype analysis: G-banding chromosome of m17.ASC cells at two passages (p 10 and p73), which was normal if compared with normal mouse karyotype (19, XX). **(b)** Population doubling time. Every 3 days $1 \times 10^5/cm^2$ of m17.ASC (from p82 to p91) and primary cells (from p1 to p10) were passaged sequentially (named p1–10 in abscissae for both cell types). **(c)** Telomere length was measured in this series of passages, as well as from p27 to p32, from p43 to p49 and from p107 to p113 and was compared with the telomere length of SVF at p1. **(d)** m17.ASCs do not display transforming activity, as assessed in a soft agar assay, which allows only anchorage-independent cell proliferation. In these conditions, m17.ASCs produced even a lower number of colonies relative to NIH-3T3 cells used as a negative control. By contrast, transformed NIH-3T3-Met-EC$^-$ gave a high number of colonies. Representative experiments out of the three performed are reported. SVF, stromal vascular fraction.

10-fold change. Additional probes gave detectable signals in both cells but at different levels: 481 with more than 3-fold change (238 up- and 243 down-regulated in m17.ASCs) and 41 with more than 10-fold change (23 up- and 18 down-regulated in m17.ASCs; see Supplementary Table S1 for full gene lists; Supplementary Data are available online at www.liebertpub.com/scd). The four categories of differentially expressed genes are illustrated in Figure 4a. From the data provided earlier, it can be concluded that about 2.5% of the genes underwent an expression change or gain/loss of >3-fold, and only 0.4% of the genes was more than 10-fold changed. The fact that more genes were lost than gained is not surprising, as the SVF is more heterogeneous than the clonal m17.ASC line.

m17.ASCs were found to up-regulate or ex-novo acquire the expression of genes positively regulating cell growth or other activities that were usually found to be associated with stem and progenitor cells, such as migration and morphogenesis (ie, UP: *Histones Egln3, Hist1h2an, Hist1h2ak, Hist1h2ao, Mdk, Rpl29, Tgfbi*; GAINED: *Esm1, 9230117N10Rik, Mcm6, Cxcl12, Ercc5, Gcnt1, and Enpp2*).

Conversely, these cells were found to down-regulate or lose the expression of genes negatively regulating the cell cycle [ie, DOWN: *nhba, Cryab, Gadd45g* (-8.96), *Il11*, LOST: *IL-11*, *Cxcl14, Gas6, H19,* and *cdkn1c*]. Moreover, m17.ASCs down-regulated or lost the expression of genes involved in specific cell-differentiated phenotypes, such as the keratins and different junctional proteins that are typical of epithelial tissues (*Krt1-14*, *Krt1-17*, *krt7*, *cldn4*, and *Gjb3*) or axon guidance and typical of nervous tissues (*Sema7a, Ncam*).

An in-depth gene analysis was carried on to disclose whether genes related to immortalization, such as *c-myc, bcl2, cyclin D*, and telomerase, were up-regulated in m17.ASC cells as well. However, no evidence emerged in favor of this possibility, with their expression level being the same in the three cell types tested (*Ccnd1*: high; c-Myc: medium-low; *bcl-2*: low; *mTert*: negative) (data not shown). A similar analysis was performed relative to the up-regulation of oncogenes (*Wnt* family, *Fzd* family, *Stat* family, and *HIF1*) and the down-regulation of tumour suppressor genes (*Rb, p53*) and in this case also, no clear evidence was found for changes between the three cell types, because oncogenes were generally found to be expressed from very low to medium levels and tumor suppressor genes were found to be always expressed at medium-low or medium-high levels (data not shown).

Due to the relevance in obtaining cells to be adopted for cardiac tissue engineering, and the difficulty in culturing adult mesenchymal stem cells, SVF were cultured in a medium suited for cardiomyocytes. On this basis, we expected that the clone could acquire signatures of cardiac cells. We, thus, carried out expression profiles also of nCM

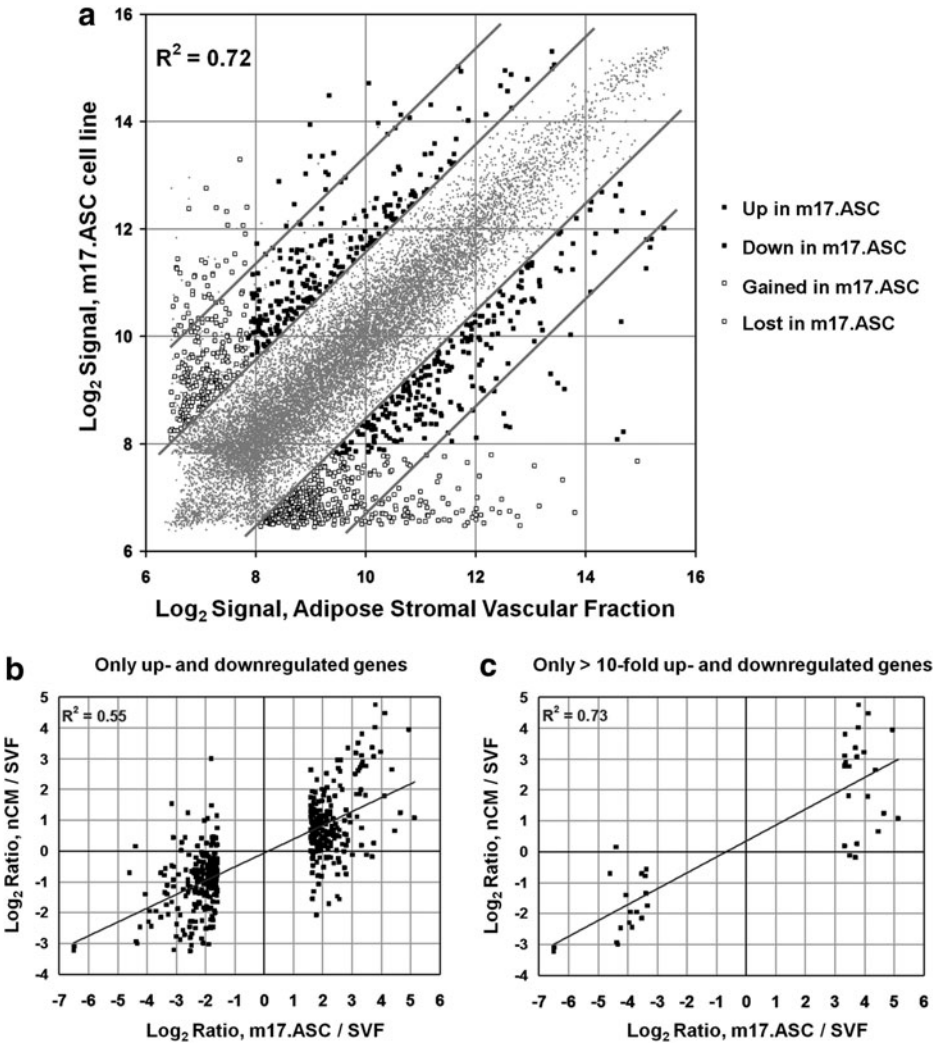

FIG. 4. Gene expression profile. **(a)** Genes displaying gain (■, *left*), loss (■, *right*) or differential expression (□, up-regulated on the *left* and □, down-regulated on the *right*) in m17.ASC cells (vertical axis) compared with the SVF derived from subcutaneous adipose tissue (SVF, horizontal axis) by microarray. The scatterplot shows normalized microarray datasets of m17.ASC and SVF. All 45,281 gene probes are represented in this plot. **(b)** Gene expression changes in m17.ASC and nCM versus SVF are correlated. Genes previously selected for up- and down-regulation in m17.ASCvs SVF cells are plotted for their m17.ASC/SVF log2 ratio expression on the x-axis, and their nCM/SVF Log2 ratio expression on the y-axis. nCM, neonatal cardiomyocytes.

preparations for a comparison. Indeed, the m17.ASC transcriptome turned out to be more correlated to nCMs ($R^2 = 0.87$) than to SVF ($R^2 = 0.80$). Interestingly, as illustrated in Fig. 4b, expression changes between m17.ASC and SVF cells were found to be highly correlated to expression changes observed between nCMs and SVF, in particular when genes with more than a 10-fold change between m17.ASC and SVF were selected ($R^2 = 0.73$; Fig. 4c). These data indicate that long-term culture in specific conditions can drive partial commitment toward the cardiomyocyte phenotype, although further stimuli are required for a complete differentiation.

The m17.ASC line can engraft in NOD/SCID-γ ^{null} mice

In regenerative medicine, the ultimate goal is to transplant cells that are capable of engrafting in vivo, proliferating, and providing a therapeutic benefit. In order to explore the in vivo properties of GFP-m17.ASC, NOD/SCID-γ ^{null} mice, in which adaptative immune response is lacking and innate immune response is impaired, and, thus, GFP-positive cells should not be rejected by the immune system, were transplanted with these cells by an intrasplenic injection. At different time points, animals were killed, and their liver sections were processed for immunofluorescence staining with anti-GFP and anti-CD31 antibodies. Cells were engrafted and persisted until 6 weeks, the longest time tested, and could be found in the liver parenchyma and in the proximity of vessels (Fig. 5), a location that corresponds to their original location in the stromal adipose tissue from where they originated. A few cells were found to be positive for CD31, a recognized endothelial cell marker. It can, thus, be concluded that m17.ASC cells can engraft in vivo, persist there for at least 6 weeks, and start to differentiate toward an endothelial phenotype.

Discussion

Adult stem cells are a key component for regenerative medicine. The aim of the researchers involved in regenerative medicine is to reproduce the right environment, mimicking as much as possible the in vivo situation of a living organism, where tissues are formed and renewed under the influence of spatially and temporally orchestrated physical and chemical stimuli [24].

In vitro tissue engineering is a relatively young discipline, and, although great advances have been obtained, many

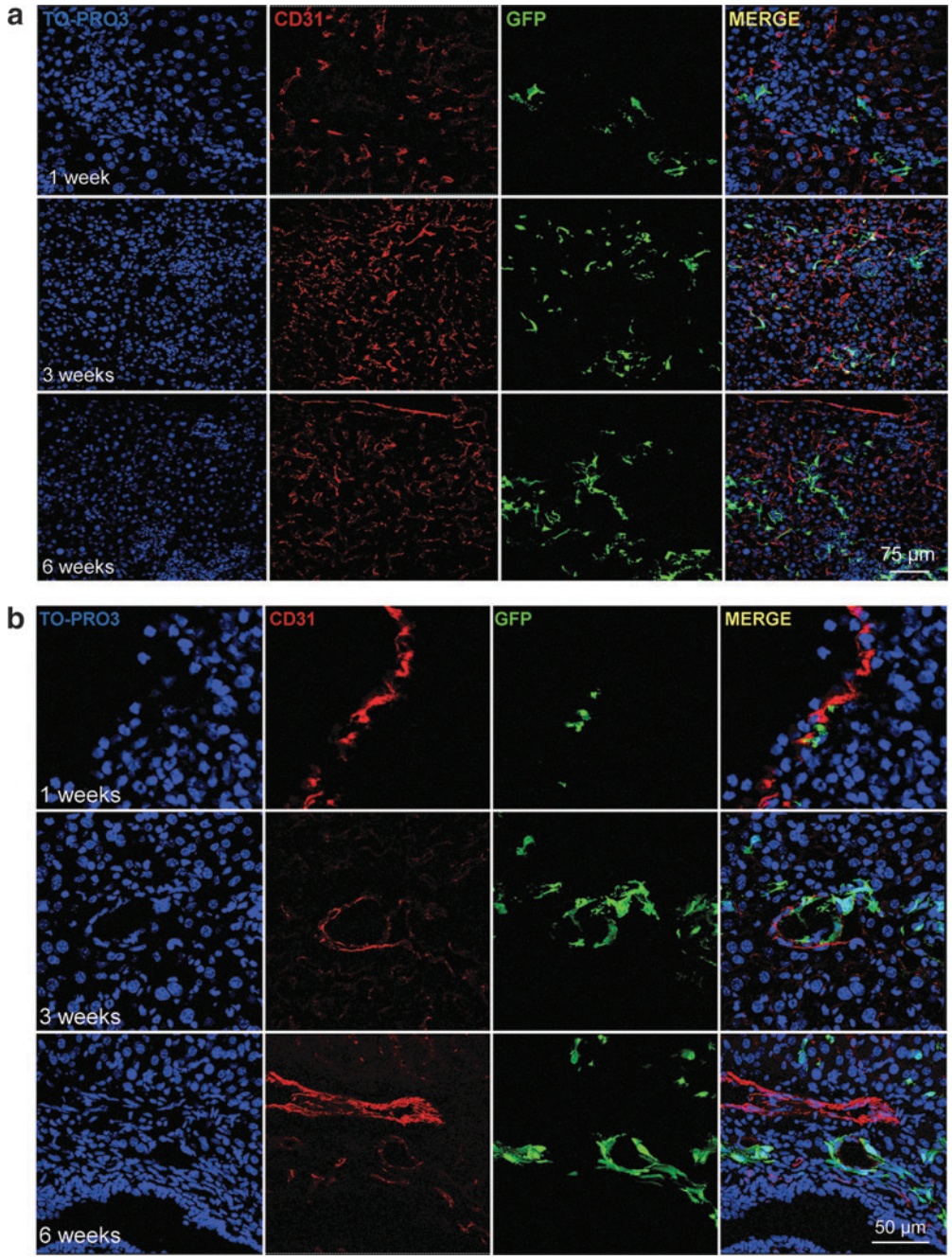

FIG. 5. m17.ASCs engraft in NOD/SCID-γ^{null} mice. GFP-m17.ASCs in liver sinusoids after intrasplenic injection. Liver sections from mice killed after different time points were stained for GFP (*green*), TO-PRO3 (*blue*), and CD31 (*red*) and analyzed by confocal microscopy, singly or after merging. Cell engraftment was analyzed at 1, 3, and 6 weeks after transplantation and are reported at two different enlargements **(a:** original magnification 400×; **b:** original magnification 950×**)**. One representative experiment out of three performed is reported (two animals per group per experiment). GFP, green fluorescent protein. Color images available online at www.liebertpub.com/scd

investigations are going on to refine and improve these complex biomimetic constructs. Many materials are being developed for scaffolds for a structural substrate and are able to release mechanical and structural signals. The role of scaffold design is particularly evident when stem/progenitor cells are used to fabricate architecturally complex tissues, such as the myocardium [25,26,32]. It is, thus, clear that the advantage is to have a standardized and easily available source of stem cells endowed with multipotency, which can be unlocked and guided toward specific histotypes by the physical and chemical cues provided by the environment in which they are cultured in vitro. The studies involving stem cells usually require a significant amount of primary cells and an extensive in vitro expansion. Adult stem cells are particularly difficult to expand and keep in culture for a long time, even those from adipose tissue, and although different

culture conditions have been suggested by many researchers [3,5,47], no continuous lines with these properties have been established.

Here, the properties and some of the possible applications of cells, named m17.ASC, stabilized with appropriate culture conditions from a clone of spontaneously immortalized murine adult mesenchymal stem cells, are reported. The m17.ASCs originated from cultures of the SVF of adipose tissue, selected for the expression of the stemness marker Sca-1. This cell line has been fully characterized, and both in vitro and in vivo behaviors have been described. The peculiar characteristics of m17.ASC have been analyzed in their complex in order to prove its potential and safety. The main peculiarities of m17.ASC which are described are their stemness properties, that is, indefinite self-renewal and multipotency. Stem cells from murine adipose tissue, as well as from bone marrow, usually undergo senescence within a few culture passages. To overcome this limit, some authors have proposed to immortalize cells from bone marrow with mTERT, thus inducing constitutive telomerase activity and telomere elongation [49–51]. However, these cells also acquired transformed and tumorigenic activities, when inoculated in syngeneic recipient animals [16,18,52]. By contrast, m17.ASCs behave in a normal manner, as testified by their inability to proliferate in anchorage-independent conditions or as tumors in NOD/SCID-γ^{null} mice, although they are able to maintain a stable proliferation, probably sustained by a substantial telomere stability. Moreover, both the karyotype and gene expression analyses did not demonstrate any typical tumor-associated alteration. In line with the not-transformed or tumorigenic properties of m17.ASC cells, global gene expression analysis revealed that neither up-regulation of oncogenes nor down-regulation of tumor suppressor genes was detectable. These data strongly exclude the mechanisms described above as causative of m17.ASC immortalization.

Although m17.ASCs did not grow as tumors in NOD/SCID-γ^{null} mice, they could engraft in the liver when transplanted in vivo through an intraspleenic injection and persisted there for at least 6 weeks, the last time point examined, in which the number of transplanted cells increased with some level of proliferation. A few cells appeared to have undertaken the differentiation pathway toward endothelial cells, as they expressed the CD31 marker. Thus, the m17.ASC maintained the multipotency typical of the SVF from which it originated, being able to differentiate in osteogenic, chondrogenic, adipogenic, and cardiogenic phenotypes in vitro, and endothelial phenotype in vivo.

In order to propose this cell line as a good source of adult stem cells that are able to stably replicate, we also analyzed whether long-term culture (to date more than 2 years of continuous culture) or cryopreservation would modify its phenotype. The results confirmed that m17.ASC maintained a stable expression of different stemness markers and substantially maintained the transcriptional features of the original SVF cells. Only a minor fraction of the sequences analyzed underwent qualitative or quantitative changes, with an increased or de novo expression of genes positively regulating cell growth or other activities that are usually found to be associated with stem/progenitor cells, such as migration and morphogenesis, and a decreased or lost expression of genes involved in specific differentiated cell phenotypes. As already discussed, evidence of neither up-regulation of oncogenes nor down-regulation of tumor suppressor genes was detected.

Telomere length displayed some variability, which, however, was in the range of the one observed in the SVF at their first passages. This finding is congruent with what is observed in stem or progenitor cells, such as germinal cells, and is indicative of the telomere maintenance [53]. On the contrary, in most cancer cells with a high or low proliferation rate, telomere length is greatly reduced or significantly elongated, respectively, due to a constitutive expression of telomerase [54].

The successful stabilization of the clone might also be due to the particularly rich culture medium used, originally developed for cardiomyocytes. For this reason, cells acquired an expression profile that was somehow closer to nCMs, still maintaining, however, their multipotency.

m17.ASC displays a typical fibroblastoid morphology and expresses the stemness markers Sca-1, c-Kit/CD117, nestin, nucleostemin, CD44, and CD106, but did not express the embryonal stemness markers Nanog, Oct4, and Sox2. Among the stemness markers tested, CD90 was found to be expressed at lower levels—around 20%—than generally reported for adipose-derived mesenchymal stem cells, Similar results, however, were recently reported for mesenchymal stem cells isolated from the adipose tissue of different mouse strains [55], and, indeed, these cells were endowed with multipotency. Due to its many properties, m17.ASC may represent a valuable tool for a number of applications in ex vivo tissue engineering, namely aimed at analyzing physical (e.g., electrical, mechanical, and topographical) or biochemical parameters (selected growth factors, hormones, and other biologically active molecules and possibly inhibiting drugs, their combination, or timing) with the advantage that it does not require repeated animal sacrifice.

Conclusion

As such, this cell line is an excellent candidate that could be used for investigating the requirements in terms of biomolecules, their combination, or timing, as well as of scaffolds in tissue engineering and regenerative medicine. Moreover, it can be used as a platform to test the effects of drugs in the differentiation induction process. Future studies would investigate whether m17.ASC could be induced to osteoblastic differentiation when plated on titanium scaffolds. Indeed, preliminary data suggest that they can be suitable to test unconventional cell culture substrates for tissue engineering.

Acknowledgments

The authors are grateful to Andrea Sprio for helpful discussion, to Daniela Cantarella for technical assistance with gene expressing profile, and to Roberto Serra for helping in editing this article. This work was supported by Cariplo Foundation (grant 2008–2459), Regione Piemonte (Ricerca sanitaria finalizzata grant 2008–2981) to M.P. and PRIN 2008, and Telethon GGP09280 to A.F.

Author Disclosure Statement

M. Prat, S. Pietronave, A. Zamperone, research agreement with the Università del Piemonte Orientale, and Patent Appl.

No. US 13/309,132 filed on Dec. 1, 2011 related to U. S. Provisional application No. 61/344,973, filed on Dec. 1, 2010. The authors acknowledge the cooperation of MITO Technology srl, as it has signed a Deposit License Agreement with Health Protection Agency Culture Collection (HPACC) on November 15, 2011 for the preservation and distribution of the new cell line.

References

1. Pittenger MF, AM Mackay, SC Beck, RK Jaiswal, R Douglas, JD Mosca, MA Moorman, DW Simonetti, S Craig and DR Marshak. (1999). Multilineage potential of adult human mesenchymal stem cells. Science 284:143–147.
2. Zuk PA. (2010). The adipose-derived stem cell: looking back and looking ahead. Mol Biol Cell 21:1783–1787.
3. Schäffler A and C Bűchler. (2007). Concise review: adipose tissue-derived stromal cells–basic and clinical implications for novel cell-based therapies. Stem Cells 25:818–827.
4. Gimble JM, AJ Katz and BA Bunnell. (2007). Adipose-derived stem cells for regenerative medicine. Circ Res 100: 1249–1260.
5. Lindroos B, R Suuronen and S Miettinen. (2011). The potential of adipose stem cells in regenerative medicine. Stem Cell Rev 7:269–291.
6. Kern S, H Eichler, J Stoeve, H Klüter and K Bieback. (2006). Comparative analysis of mesenchymal stem cells from bone marrow umbilical cord blood or adipose tissue. Stem Cells 24:1294–1301.
7. Toyoda M, Y Matsubara, K Lin, K Sugimachi and M Furue. (2009). Characterization and comparison of adipose tissue-derived cells from human subcutaneous and omental adipose tissues. Cell Biochem Funct 27:440–447.
8. Nakanishi C, N Nagaya, S Ohnishi, K Yamahara, S Takabatake, T Konno, K Hayashi, MA Kawashiri, T Tsubokawa and M Yamagishi. (2011). Gene and protein expression analysis of mesenchymal stem cells derived from rat adipose tissue and bone marrow. Circ J 75:2260–2268.
9. Helder MN, M Knippenberg, J Klein-Nulend and PI Wuisman. (2007). Stem cells from adipose tissue allow challenging new concepts for regenerative medicine. Tissue Eng 13:1799–1808.
10. Liu TM, M Martina, DW Hutmacher, JH Hui, EH Lee and B Lim. (2007). Identification of common pathways mediating differentiation of bone marrow and adipose tissue-derived human mesenchymal stem cells into three mesenchymal lineages. Stem Cells 25:750–760.
11. Roche R, L Hoareau, F Mounet and F Festy. (2007). Adult stem cells for cardiovascular diseases: the adipose tissue potential. Expert Opin Biol Ther 7:791–798.
12. Saulnier N, MA Puglisi, W Lattanzi, L Castellini, G Pani, G Leone, S Alfieri, F Michetti, AC Piscaglia and Gasbarrini A. (2011). Gene profiling of bone marrow and adipose tissue-derived stromal cells: a key role of Kruppel-like factor 4 in cell fate regulation. Cytotherapy 13:329–340.
13. Gronthos S, DM Franklin, HA Leddy, PG Robey, RW Storms and JM Gimble. (2001). Surface protein characterization of human adipose tissue-derived stromal cells. J Cell Physiol 189:54–63.
14. Gimble JM, F Guilak and BA Bunnell. (2010). Clinical and preclinical translation of cell-based therapies using adipose tissue-derived cells. Stem Cell Res Ther 1:19–29.
15. Mizuno H, M Tobita and AC Uysal. (2012). Concise review: adipose-derived stem cells as a novel tool for future regenerative medicine. Stem Cells 30:804–810.
16. Casalbore P, M Budoni, L Ricci-Vitiani, C Cenciarelli, G Petrucci, L Milazzo, N Montano, E Tabolacci, G Maira, LM Larocca and Pallini R. (2009). Tumorigenic potential of olfactory bulb-derived human adult neural stem cells associates with activation of TERT and NOTCH1. PLoS One 4:e4434.
17. Li H, X Fan, RC Kovi, Y Jo, B Moquin, R Konz, C Stoicov, E Kurt-Jones, SR Grossman, et al. (2007). Spontaneous expression of embryonic factors and p53 point mutations in aged mesenchymal stem cells: a model of age-related tumorigenesis in mice. Cancer Res 67:10889–10898.
18. Chen BY, X Wang, LW Chen and ZJ Luo. (2012). Molecular targeting regulation of proliferation and differentiation of the bone marrow-derived mesenchymal stem cells or mesenchymal stromal cells. Curr Drug Targets 13:561–571.
19. Qin Y, H Ji, Y Wu and H Liu. (2009). Chromosomal instability of murine adipose tissue-derived mesenchymal stem cells in long-term culture and development of cloned embryos. Cloning Stem Cells 11:445–452.
20. Yuan HF, C Zhai, XL Yan, DD Zhao, JX Wang, Q Zeng, L Chen, X Nan, LJ He, et al. (2012). SIRT1 is required for long-term growth of human mesenchymal stem cells. J Mol Med (Berl) 90:389–400.
21. Ning H, G Liu, G Lin, M Garcia, LC Li, TF Lue and CS Lin. (2009). Identification of an aberrant cell line among human adipose tissue-derived stem cell isolates. Differentiation 77:172–180.
22. Williams BR, VR Prabhu, KE Hunter, CM Glazier, CA Whittaker, DE Housman and A Amon. (2008). Aneuploidy affects proliferation and spontaneous immortalization in mammalian cells. Science 322:703–709.
23. Knoepfler PS. (2009). Deconstructing stem cell tumorigenicity: a roadmap to safe regenerative medicine. Stem Cells 27:1050–1056.
24. Langer R and JP Vacanti. (1993). Tissue engineering. Science 260:920–926.
25. Freed LE, F Guilak, XE Guo, ML Gray, R Tranquillo, JW Holmes, M Radisic, MV Sefton, D Kaplan and G Vunjak-Novakovic. (2006). Advanced tools for tissue engineering: scaffolds bioreactors and signalling. Tissue Eng 12:3285–3305.
26. Dvir T, BP Timko, DS Kohane and R Langer. (2011). Nanotechnological strategies for engineering complex tissues. Nat Nanotechol 6:13–22.
27. Sekine H, T Shimizu and T Okano. (2012). Myocardial tissue engineering: toward a bioartificial pump. Cell Tissue Res 347:775–782.
28. Miyahara Y, N Nagaya, M Kataoka, B Yanagawa, K Tanaka, H Hao, K Ishino, H Ishida, T Shimizu, et al. (2006). Monolayered mesenchymal stem cells repair scarred myocardium after myocardial infarction. Nat Med 12:459–465.
29. Asakawa N, T Shimizu, Y Tsuda, S Sekiya, T Sasagawa, M Yamato, F Fukai and T Okano. (2010). Pre-vascularization of *in vitro* three-dimensional tissues created by cell sheet engineering. Biomaterials 31:3903–3909.
30. Lund AW, B Yener, JP Stegemann and GE Plopper. (2009). The natural and engineered 3D microenvironment as a regulatory cue during stem cell fate determination. Tissue Eng Part B Rev 15:371–380.
31. Forte G, S Pietronave, G Nardone, A Zamperone, E Magnani, S Pagliari, F Pagliari, C Giacinti, C Nicoletti, et al.

(2011). Human cardiac progenitor cell grafts as unrestricted source of supernumerary cardiac cells in healthy murine hearts. Stem Cells 29:2051–2061.
32. Pagliari S, AC Vilela-Silva, G Forte, F Pagliari, C Mandoli, G Vozzi, S Pietronave, M Prat, S Licoccia, et al. (2011). Co-operation of biological and mechanical signals in cardiac progenitor cell differentiation. Adv Mater 23:514–518.
33. Neofytou EA, E Chang, B Patlola, LM Joubert, J Rajadas, SS Gambhir, Z Cheng, RC Robbins and RE Beygui. (2011). Adipose tissue-derived stem cells display a proangiogenic phenotype on 3D scaffolds. J Biomed Mater Res A 98:383–393.
34. Santo VE, AR Duarte, EG Popa, ME Gomes, JF Mano and RL Reis. (2012). Enhancement of osteogenic differentiation of human adipose derived stem cells by the controlled release of platelet lysates from hybrid scaffolds produced by supercritical fluid foaming. J Control Release 162:19–27.
35. Rodrigues AI, ME Gomes, IB Leonor and RL Reis. (2012). Bioactive starch-based scaffolds and human adipose stem cells are a good combination for bone tissue engineering. Acta Biomater 8:3765–3776.
36. Shi Z, KG Neoh, ET Kang, CK Poh and W Wang. (2012). Enhanced endothelial differentiation of adipose-derived stem cells by substrate nanotopography. J Tissue Eng Regen Med [Epub ahead of print]; DOI: 101002/term1496.
37. Shi JG, WJ Fu, XX Wang, YD Xu, G Li, BF Hong, Y Wang, ZY Du and X Zhang. (2012). Tissue engineering of ureteral grafts by seeding urothelial differentiated hADSCs onto biodegradable ureteral scaffolds. J Biomed Mater Res A 100:2612–2622.
38. Li H, Y Xu, Q Fu and C Li. (2012). Effects of multiple agents on epithelial differentiation of rabbit adipose-derived stem cells in 3D. Culture Tissue Eng Part A 18:1760–1770.
39. Ogushi Y, S Sakai and K Kawakami. (2012). Adipose tissue engineering using adipose-derived stem cells enclosed within an injectable carboxymethylcellulose-based hydrogel. J Tissue Eng Regen Med [Epub ahead of print]; DOI: 101002/term1480.
40. Choi JS, BS Kim, JD Kim, YC Choi, HY Lee and YW Cho. (2012). *In vitro* cartilage tissue engineering using adipose-derived extracellular matrix scaffolds seeded with adipose-derived stem cells. Tissue Eng Part A 18:80–92.
41. von Figura G, D Hartmann, Z Song and KL Rudolph. (2009). Role of telomere dysfunction in aging and its detection by biomarkers. J Mol Med (Berl) 87:1165–1171.
42. Cristofalo VJ, RG Allen, RJ Pignolo, BG Martin and JC Beck. (1998). Relationship between donor age and the replicative lifespan of human cells in culture: a reevaluation. Proc Natl Acad Sci U S A 95:10614–10619.
43. Merlin S, S Pietronave, D Locarno, G Valente, A Follenzi and M Prat. (2009). Deletion of the ectodomain unleashes the transforming invasive and tumorigenic potential of the MET oncogene. Cancer Sci 100:633–638.
44. Callicott RJ and JE Womack. (2006). Real-time PCR assay for measurement of mouse telomeres. Comp Med 56:17–22.
45. Yamakawa K, H Iwasaki, I Masuda, Y Ohjimi, I Honda, K Saeki, J Zhang, E Shono, M Naito and M Kikuchi. (2003). The utility of alizarin red s staining in calcium pyrophosphate dihydrate crystal deposition disease. J Rheumatol 30:1032–1035.
46. Sprio AE, F Di Scipio, S Raimondo, P Salamone, F Pagliari, S Pagliari, A Folino, G Forte, S Geuna, P Di Nardo and GN Berta. (2012). Self-renewal and multipotency coexist in a long-term cultured adult rat dental pulp stem cell line: an exception to the rule? Stem Cells Dev [Epub ahead of print]: DOI: 101089/scd20120141.
47. Committee on Standardized Genetic Nomenclature For Mice—Standard Karyotype of the Mouse *Mus musculus*. (1972). J Hered 63:69–72.
48. Follenzi A, D Benten, P Novikoff, L Faulkner, S Raut S and S Gupta. (2008). Transplanted endothelial cells repopulate the liver endothelium and correct the phenotype of hemophilia A mice. J Clin Invest 118:935–945.
49. Thi MM, M Urban-Maldonado, DC Spray and SO Suadicani. (2010). Characterization of hTERT-immortalized osteoblast cell lines generated from wild-type and connexin43-null mouse calvaria. Am J Physiol Cell Physiol 299:994–1006.
50. Kogan I, N Goldfinger, M Milyavsky, M Cohen, I Shats, G Dobler, H Klocker, B Wasylyk, M Voller, et al. (2006). hTERT-immortalized prostate epithelial and stromal-derived cells: an authentic *in vitro* model for differentiation and carcinogenesis. Cancer Res 66:3531–3540.
51. Boklan J, G Nanjangud, KL MacKenzie, C May, M Sadelain and MA Moore. (2002). Limited proliferation and telomere dysfunction following telomerase inhibition in immortal murine fibroblasts. Cancer Res 62:2104–2114.
52. Yamaoka E, E Hiyama, Y Sotomaru, Y Onitake, I Fukuba, T Sudo, T Sueda and K Hiyama. (2011). Neoplastic transformation by TERT in FGF-2-expanded human mesenchymal stem cells. Int J Oncol 39:5–11.
53. Collins K and JR Mitchell. (2002). Telomerase in the human organism. Oncogene 21:564–579.
54. Kim NW, MA Piatyszek, KR Prowse, CB Harley, MD West, PL Ho, GM Coviello, WE Wright, SL Weinrich and JW Shay. (1994). Specific association of human telomerase activity with immortal cells and cancer. Science 266:2011–2015.
55. Pazdro R and DE Harrison. Murine adipose tissue-derived stromal cell apoptosis and susceptibility to oxidative stress *in vitro* are regulated by genetic background. PLoS One 2013;8:e61235.

Address correspondence to:
Maria Prat
Dipartimento di Scienze della Salute
Università del Piemonte Orientale
Via Solaroli 17
28100 Novara
Italy

E-mail: mprat@med.unipmn.it

Received for publication December 27, 2012
Accepted after revision June 13, 2013
Prepublished on Liebert Instant Online June 18, 2013